

A Gain/Phase Imbalance Minimization Technique for LINC Transmitter

Xuejun Zhang, Peter Nanawa, Lawrence E. Larson, and Peter M. Asbeck

Center for Wireless Communications, University of California, San Diego, La Jolla, CA 92093

Abstract — A simple calibration scheme for correction of the path imbalance in a LINC transmitter has been demonstrated. In this algorithm a baseband DSP evaluates the gain and phase imbalance with a set of calibration signals through a feedback loop. Compensation of path imbalance is accomplished within the DSP by introducing a pre-distortion term. The quadrature errors of the I/Q modulators set a limit on the overall performance of this algorithm. A prototype LINC system has been tested for CDMA IS95 baseband input and -38 dBc ACI was achieved.

I. INTRODUCTION

The outphased power amplifier concept dates back to the early 1930's as an approach for the simultaneous realization of high-efficiency and high-linearity amplification. It has been revived recently for wireless communication applications under the rubric of LINC (linear amplification with nonlinear components) [1]; many recent papers have developed the concept further [2]-[3], including a variation called CALLUM [4]. The LINC concept takes an envelope modulated bandpass waveform and resolves it into two out-phased constant envelope signals, which are applied to highly efficient — and highly nonlinear — power amplifiers, whose outputs are summed. The advantage of this approach is that each amplifier can be operated in a very power efficient mode, and the final output can be highly linear and free of intermodulation — a key consideration for bandwidth efficient wireless communications.

One of the major disadvantages of this technique is the extremely tight tolerance on the matching of the two amplifier paths to achieve acceptably small out-of-band rejection. This problem has been analyzed by a number of authors, and the typical requirements for most practical applications are approximately 0.1-0.5 dB in gain matching or 0.4-2° in phase matching, depending on the modulations. This is nearly impossible to achieve in most practical situations, and several attempts have been made to correct for the errors. A “phase-only” correction was proposed in [5]. A simplex search algorithm was proposed in [6] to correct for both gain and phase errors. This algorithm requires a long data sequence for the measurement of the out-of-band emission, which sets a

lower limit on the calibration time of around 1-2 seconds. A direct search method was proposed in [7] to correct the gain imbalance as well as the consequent phase imbalance due to AM-PM transition. A method was presented in [8], in which path imbalance and quadrature imbalance are characterized by a few RF power measurements at different locations. We have proposed a calibration scheme in [9]. In this approach the evaluation of path imbalance is based on the measurement on a set of down-converted and low-pass filtered calibration signals. The detailed analysis and simulation results can be found in that paper. A brief description of this algorithm with experimental results is given in the following sections.

II. LINC CALIBRATION ALGORITHM

A complex representation of the band-limited source signal can be written as

$$s(t) = a(t)e^{j\theta(t)}; \quad 0 \leq a(t) \leq V_m \quad (1)$$

This signal is split by the SCS (signal component separator) into two signals with modulated phase and constant amplitude.

$$\begin{aligned} S_1(t) &= s(t) - e(t) \\ S_2(t) &= s(t) + e(t) \end{aligned} \quad (2)$$

The quadrature signal $e(t)$ is defined by

$$e(t) = js(t)\sqrt{\frac{V_m^2}{a^2(t)} - 1} \quad (3)$$

The two signals are then amplified individually and sent to a hybrid combiner, as shown in Fig. 1. Note that two balanced modulators are employed to translate the baseband signal to desired carrier frequency. If two amplifier paths are perfectly matched, the in-phase signal components add in power and the out-of-phase components cancel each other; the resultant signal is the desired amplified replica of the original signal. In practice, however, this condition is difficult to achieve. In contrast to the narrowband source signal $s(t)$, the

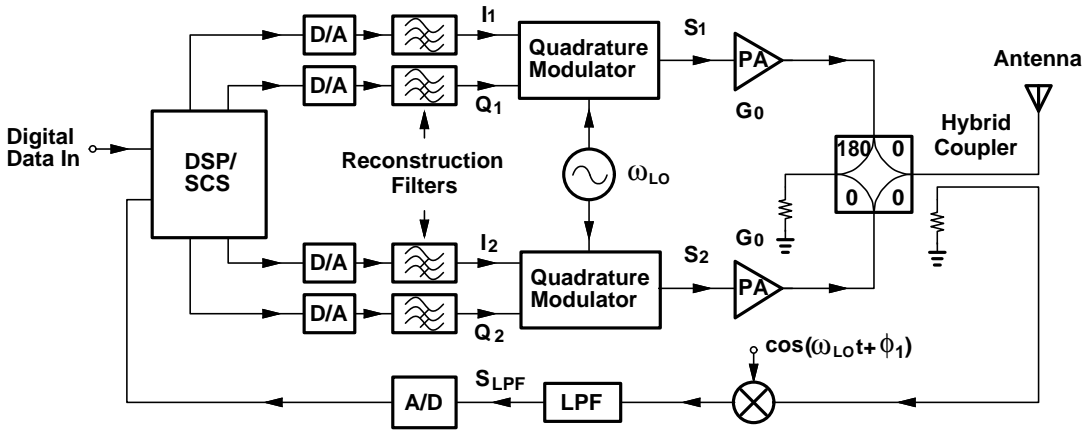


Fig. 1 LINC transmitter with calibration loop.

spectrum of $e(t)$ extends far into adjacent channels [6], and the incomplete cancellation of wideband components leaves a residue in adjacent channels, hence introducing ACI (adjacent channel interference).

The improved LINC system makes use of the standard of amplitude and phase produced by the DSP to calibrate the amplifiers through a feedback loop, as is illustrated in Fig. 1. While the DSP generates the calibration signals, a small portion of the power is withdrawn by a directional coupler. This signal is then down-converted, low-pass filtered, A/D converted and finally sent back to the DSP. The DSP extracts the gain and phase imbalance, and eliminates the error effects by introducing a correction term. As a matter of fact, the DSP modulates and filters the original baseband signal, and compensates the gain and phase imbalance --- the SCS is part of its function. Suppose that the gain and phase imbalance of the lower amplifier with respect to the upper one are $\Delta G/G_0$ and $\Delta\phi$, respectively, the signal after low-pass filter can be expressed as

$$S_{LPF} = \frac{1}{2} G_L V_m \{ \cos[\theta(t) - \psi(t) + \phi] + (1 + \frac{\Delta G}{G_0}) \cos[\theta(t) + \psi(t) + \phi + \Delta\phi] \} \quad (4)$$

where $\cos[\psi(t)] = a(t)/V_m$. G_L is the effective gain of the whole loop. ϕ includes phase delay of the calibration loop and phase shift introduced by downconversion mixer.

The correction algorithm consists of several steps. First, we set the amplitude of the input baseband signal to the maximum allowable level of the SCS, i.e., $a(t) = V_m$. Then setting $\theta(t) = 0$, which means $I_1 = I_2 = V_m$ and $Q_1 = Q_2 = 0$. After dropping off higher order terms, the result is

$$S_0 \approx G'_L V_m \cos(\phi + \frac{1}{2} \Delta\phi) \quad (5)$$

where $G'_L = (1 + \Delta G/2G_0)G_L$. This result S_0 is stored in the DSP. Similarly, by setting $\theta(t) = \pi/2$ and keeping $a(t) = V_m$, corresponding to $I_1 = I_2 = 0$ and $Q_1 = Q_2 = -V_m$, we get

$$S_p \approx -G'_L V_m \sin(\phi + \frac{1}{2} \Delta\phi) \quad (6)$$

We then set the amplitude of the input baseband signal to zero, i.e., $a(t) = 0$. As before, we set $\theta(t) = 0$, i.e., $I_1 = I_2 = 0$, $Q_1 = V_m/2$ and $Q_2 = -V_m/2$, to obtain S_a , and set $\theta(t) = \pi/2$, i.e., $I_1 = V_m/2$, $I_2 = -V_m/2$ and $Q_1 = Q_2 = 0$, to obtain S_b . From (4), (5) and (6), we may write S_a and S_b in matrix form as

$$\begin{pmatrix} S_a \\ S_b \end{pmatrix} \approx -\frac{1}{2} \begin{pmatrix} -S_p & S_0 \\ S_0 & S_p \end{pmatrix} \begin{pmatrix} \Delta G/G_0 \\ \Delta\phi \end{pmatrix} \quad (7)$$

Solving (7) for $\Delta G/G_0$ and $\Delta\phi$ yields

$$\begin{aligned} \frac{\Delta G}{G_0} &\approx \frac{1}{P_L} (S_p S_a - S_0 S_b) \\ \Delta\phi &\approx -\frac{1}{P_L} (S_0 S_a + S_p S_b) \end{aligned} \quad (8)$$

where $P_L = (G_L V_m)^2/2$ stands for the “average” power level normalized to a 1Ω characteristic impedance during calibration, and can be computed by

$$P_L \approx \frac{1}{2} (S_0^2 + S_p^2) \quad (9)$$

(7) indicates that the gain and phase imbalance are solely determined by S_0 , S_p , S_a and S_b . The relationships among them as well as P_L and ϕ are best illustrated in Fig. 2 in the case of small gain and phase imbalance, where S_a and S_b are the linear combinations of S_0 and S_p scaled by the gain and phase imbalance.

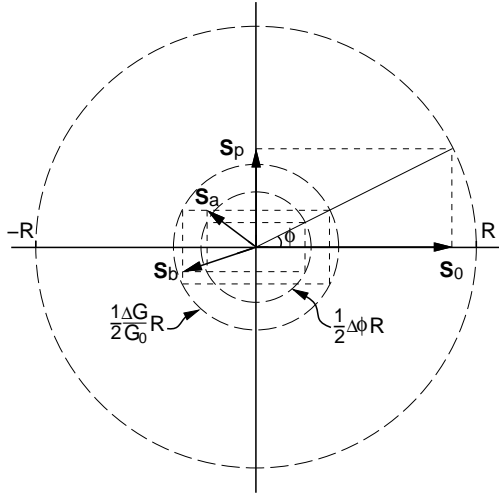


Fig. 2. Relationship between path imbalance and calibration signals. $R = G_L V_m$.

The approximations in (5), (6) and (7) give rise to a certain amount of estimation error for the measurement of the gain and phase imbalance. Note, however, that the estimation error reduces to zero as gain and phase imbalance decrease to zero. This implies that these approximations are effective in the sense that the estimate and compensation of gain and phase imbalance are iterative; with several iterations, the gain and phase imbalance are able to converge to an acceptable low level [9]. Besides, since the accuracy of P_L is not critical in determining path imbalance, the evaluation of this quantity only need to be done once, further simplifying the algorithm.

III. MEASURED RESULTS AND DISCUSSION

A LINC system has been constructed to demonstrate the calibration scheme. In this system, a personal computer, two arbitrary waveform generators and a digital oscilloscope are used to simulate the function of the DSP/SCS. The waveform generators and oscilloscope are ISA cards plugged into computer's expansion slots. Two waveform generators are synchronized to generate four channel outputs. The power amplifier has nominal 29 dBm of 1 dB compression point and 27 dB of gain. The upper amplifier operates at the gain compressed by 2 dB. In order to adjust the power of the bottom branch, the bottom amplifier operates 3 dB backed off from the 1 dB compression point. The maximum capable output power of this system is 31 dBm.

Because very limited memory size is available in the waveform generator, the filtered PN (pseudo-noise) sequences are used as the baseband sources. The baseband filters were designed to meet CDMA IS-95

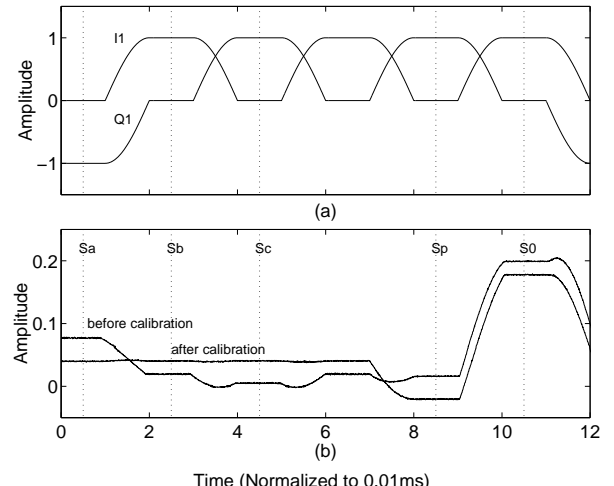


Fig. 3. (a) Calibration signal waveforms I_1 and Q_1 . (b) The snapshots before/after calibration from oscilloscope.

specifications. The waveform generators simply repeat the filtered PN sequences — no spurs will be generated. The chip rate is 1.23 Mbps and the carrier frequency is 850 MHz.

The experiment starts with a calibration, in which two arbitrary waveform generators generate four-channel synchronized calibration signals. At the same time a snapshot is taken by digital oscilloscope. The gain and phase imbalance are then evaluated and stored. At the end of each iteration, the DSP/SCS recalculate the calibration signals I_2 and Q_2 to compensate the path imbalance. These steps are repeated until the measured imbalance is under certain low level, then the waveform generators load in and generate the CDMA IS-95 baseband signals with compensation.

Fig. 3(a) shows the calibration signal waveforms I_1 and Q_1 . I_2 and Q_2 are not shown here; their waveforms are time-shifted version of Q_1 and I_1 . The dash lines indicate when the DSP/SCS takes the samples of the signal after LPF. Between dash lines are the transition that can be carefully designed to minimize out-of-band spurs. The transient effect of the LPF is not crucial in this case. Note that an extra calibration signal S_c is added, which is used to determine the DC offset of the LPF and DAC. This offset adds to the measured values and degrades the measurement accuracy and iteration convergence. S_c can be chosen to be a signal which is 180° out-of-phase with any of the four calibration signals, in this example, we choose to set $a(t) = 0$ and $\theta(t) = \pi$, i.e., $I_1 = I_2 = 0$, $Q_1 = V_m$ and $Q_2 = -V_m$. From (4), the DC offset is easily determined by $V_{\text{offset}} = (S_a + S_c)/2$ and can then be subtracted from measured values. The calibration was accomplished within 2~3 iterations. Each calibration took 0.12 ms, and can be greatly reduced even less.

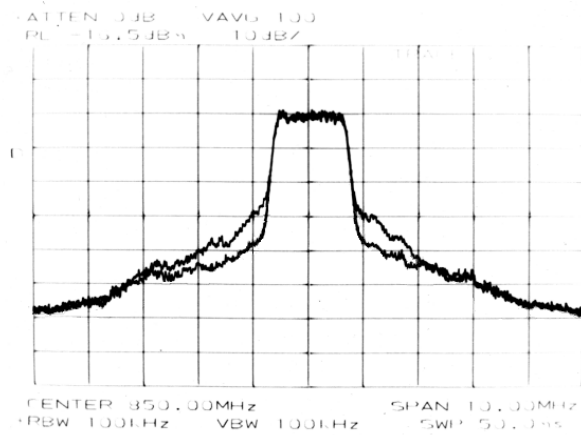


Fig.4. Measured LINC output spectra for CDMA IS95 with and without calibration.

Fig. 3(b) compares signals taken by digital oscilloscope before and after calibration. Check (7) we immediately see that for perfectly matched system, S_a , S_b and S_c should remain zero, which is consistent with the experiment. As we know, CDMA IS-95 mobile terminals transmit signal in bursts, which implies that calibration could be taken very shortly before real data transmission, with two zero-RF-power-level signals (S_a and S_b) followed by two full-RF-power-level signals (S_o and S_p) at the beginning of every few bursts.

Fig. 4 displays the output power spectrum of the LINC transmitter. Without correction, the ACI is around -27 dB, while with correction the out-of-band spectrum is suppressed efficiently below -38 dBc. Here ACI is defined as the ratio of peak spectral density of the out-of-band residue to the peak spectral density of the modulation. The measured gain and phase imbalance prior to calibration are 0.5 dB and 12°, respectively. The relatively large phase imbalance comes from the fact that the two power amplifiers work at different power levels. Considering that each modulator in our system has nominal 2° phase error and 0.3 dB gain error, and the calibrated gain and phase imbalance are [9]:

$$\frac{\Delta G}{G_0} = (g_1 - g_2) \sin \psi + (\delta_1 - \delta_2) \sin \phi \cos \phi \quad (9)$$

$$\Delta \phi = (\delta_1 - \delta_2) \cos \psi + (g_1 - g_2) \sin \phi \cos \phi$$

the -38 dBc ACI is reasonable. Here g and δ are the amplitude and phase error of the I/Q modulators, respectively. There is little we can do to minimize the effects of quadrature errors of the I/Q modulators, since these errors are random in nature. In fact the performance of this algorithm is limited by the quadrature errors.

IV. CONCLUSION

We have demonstrated a calibration technique for iterative correction of the path imbalance of the LINC transmitter. This scheme relies on the fixed standard of amplitude and phase stored in the baseband DSP to calibrate the gain and phase imbalance of the nonlinear power amplifiers. This simple scheme requires only four signal values to completely determine the imbalance at each iteration. The typically small quadrature errors determine the limit of the LINC overall performance. Experimental results confirm the analytical prediction and demonstrate that this system is sufficient to suppress the out-of-band spectrum for mobile communication applications.

ACKNOWLEDGEMENT

The authors wish to acknowledge the support by the US Army Research Office Muri-University Research Initiative Program Digital Communication Devices Based on Nonlinear Dynamics and Chaos, and the UCSD Center for Wireless Communications and its supporting member companies.

REFERENCES

- [1] D. C. Cox, "Linear amplification with nonlinear components," *IEEE Trans. Commun.*, vol. COM-23, pp. 1942-1945, Dec. 1974.
- [2] L. Couch and J. L. Walker, "VHF LINC amplifier," in *Proc. IEEE Southeastcon'82*, Destin, FL, USA, pp.122-125, 4-7 April 1982.
- [3] S. A. Hetzel, A. Bateman, and J. P. McGeehan, "LINC transmitter," *Elect. Lett.*, vol. 27, no. 10, pp. 844-846, 9 May 1991.
- [4] K. Chan and A. Bateman, "Linear modulation based on RF synthesis: realization and analysis," *IEEE Trans. Circ. Sys. I*, vol. 42, no. 6, pp. 321-333, June 1995.
- [5] S. Tomisato, K. Chiba, and K. Murota, "Phase error free LINC modulator," *Elect. Lett.*, vol. 25, no. 9, pp. 576-577, 27 April 1989.
- [6] L. Sundstrom, "Automatic adjustment of gain and phase imbalances in LINC transmitters," *Elect. Lett.*, vol. 31, no. 3, pp. 155-156, 2 Feb. 1995.
- [7] S. Ampem-Darko and H. S. Al-Raweshidy, "Gain/phase imbalance cancellation technique in LINC transmitter," *Elect. Lett.*, vol. 34, no. 22, pp. 2093-2094, Oct. 1998.
- [8] S. A. Olson and R. E. Stengel, "LINC imbalance correction using baseband preconditioning," *IEEE Radio and Wireless Conference (RAWCON 99)*, Denver, CO, pp. 179-182, Aug. 1999.
- [9] X. Zhang and L. E. Larson, "Gain and phase error free LINC transmitter," *IEEE Trans. Veh. Technol.*, vol. 49, no. 5, pp. 1986-1994, Sept. 2000.